Probe-to-Grasp Manipulation Using Self-Sensing Pneumatic Variable-Stiffness Joints

Ngoc-Duy Tran[1], Yeman Fan[1], Feng Dai[1], Khang Nguyen[2], Anh Nguyen[3], Hoang-Hiep Ly[4], Tung D. Ta[1,5], and Shigeru Chiba[1]

***Abstract*— Grasping deformable objects with varying stiffness remains a significant challenge in robotics. Estimating the local stiffness of a target object is important for determining an optimal grasp pose that enables stable pickup without damaging the object. This paper presents a probe-to-grasp manipulation framework for estimating the relative stiffness of objects using a passive soft-rigid two-finger hybrid gripper equipped with self-sensing pneumatic variable-stiffness joints. Each finger of the gripper consists of two rigid links connected by a soft pneumatic ring placed at the joint, enabling both compliant interaction and controllable joint stiffness via internal pressurization. By measuring the pressure inside the pneumatic ring, we can estimate the interaction force during contact. Building on this, we propose a practical probing strategy to infer relative object stiffness by correlating the estimated normal force with known gripper closing displacement. We validate the self-sensing model through stiffness characterization experiments across bending angles and pressure ranges, and demonstrate stiffness-aware probing-and-grasping in real-life applications: selecting grasp locations on fruits with spatially varying stiffness. The proposed system offers a minimal, low-cost sensing approach for stiffness-aware soft manipulation while retaining probing and grasping capability.**

I. INTRODUCTION

Soft robotic grippers have emerged as a promising solution for safe and adaptive manipulation, particularly when interacting with delicate and deformable objects [1]. Unlike rigid grippers, which apply relatively fixed and concentrated contact forces that may damage soft items, soft grippers inherently distribute and modulate contact forces through structural compliance. This variable-force characteristic makes them especially suitable for handling fragile objects in unstructured environments [1], [2]. However, while soft grippers can generate sufficient grasping force, accurately measuring and controlling the contact force exerted on the object remains a significant challenge. Sensory feedback is therefore essential to fully exploit the advantages of soft manipulation.

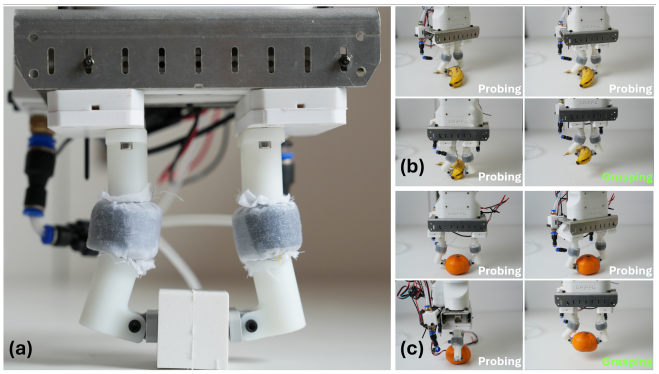


Fig. 1. Overview of the hybrid gripper mounted on a robotic arm during grasping and probing tasks. (a) The gripper integrates rigid links with a pneumatic soft-ring joint, enabling compliant interaction and variable stiffness control. (b) The hybrid gripper performs a probing process on elongated fruits, such as a banana, to estimate stiffness before grasping. (c) For round fruits such as an orange, the gripper rotates around the object to probe different locations and identify the stiffest region for a stable grasp.

Existing approaches to force estimation in soft grippers generally rely on embedded force sensors or specialized smart materials. These include piezoresistive, capacitive, and magnetic elastomer-based sensing elements integrated into the soft structure [3], [4], [5], [6]. Although effective, such solutions often increase system complexity, cost, and fabrication difficulty. Alternatively, vision-based approaches, such as marker tracking, motion capture systems, or deformation-based inference using mechanical models, have been proposed to estimate contact forces indirectly. These methods reduce hardware complexity but may require sophisticated setups or calibration procedures.

In this work, we investigate a minimal and easily deployable approach to contact force and stiffness estimation using a pressure sensor. By tracking the change in value of pressure inside a soft actuator incorporating a measured look-up data table, we estimate the interaction force without additional embedded force sensors. This setup requires only a few simple installations, significantly lowering the cost of implementation compared to conventional tactile sensing systems.

Based on the contact force estimated by the change of pressure, we further propose a strategy to infer the stiffness of the grasped object. By correlating interaction force and deformation during grasping, the system can approximate object mechanical properties without dedicated tactile arrays

*This work was supported by JSPS Grant-in-Aid for Scientific Research (B) Grant Number 23K26071, Japan, the Royal Society ISPF International Collaboration Awards 2023 (Japan) ICA\R1\231067, Hirose Foundation Research Grant, and Ministry of Education and Training (MOET) under Grant Number B2026-BKA-08 (Vietnam).

[1]Graduate School of Information Science and Technology, The University of Tokyo, Japan {duy, fanyeman, dai, tung, chiba}@csg.ci.i.u-tokyo.ac.jp

[2]Department of Robotics of the Mohamed bin Zayed University of Artificial Intelligence, UAE khang.nguyen@mbzuai.ac.ae

[3]Department of Computer Science, University of Liverpool, UK anh.nguyen@liverpool.ac.uk

[4]School of Mechanical Engineering, Hanoi University of Science and Technology, Vietnam hiep.lyhoang@hust.edu.vn

[5]Faculty of Environment and Information Studies, Keio University, Japan tung@keio.jp

or complex instrumentation.

The main contributions of this paper are as follows:

1) Proposing a passive pneumatic hybrid gripper system that enables both probing and grasping with a simple pressure system.
2) Introducing a practical strategy for estimating object stiffness based on the adjustable stiffness capability and intrinsic parameters of the pneumatic hybrid gripper.

II. RELATED WORK

Estimating object stiffness is an important problem in robotics and haptics [7]. Existing approaches can generally be categorized into absolute stiffness estimation and relative stiffness estimation. Absolute stiffness estimation aims to determine the physical stiffness parameter, typically defined as the ratio between applied force and resulting deformation according to Hooke's law. Traditional methods rely on force–displacement measurements obtained from sensors (e.g., tactile sensor, force–torque sensor, or indentation devices), where controlled probing actions are applied to derive the stiffness [8]. More recently, learning-based techniques have been explored to infer stiffness from multimodal sensory data such as force signals, tactile images, and deformation measurements [9], [10]. For example, Bednarek et al. [11] proposed a deep learning framework that estimates stiffness during squeezing using IMU signals collected from the soft gripper.

In order to achieve stiffness estimation and adaptive grasping, traditional rigid grippers typically employ multiple rigid fingers to enable accurate position and force control [12]. However, safely interacting with objects with varying mechanical properties requires compliant mechanisms and reliable force estimation capabilities. To address this challenge, Ruiz et al. [13] proposed a compliant gripper with four underactuated fingers capable of estimating grasping forces using a kinetostatic finger model, enabling safe physical human–robot interaction. Beyond specialized hardware, recent work has explored leveraging intrinsic sensing within robotic grippers to infer contact conditions without external sensors. For instance, Cortinovis et al. [14] developed algorithms that detect finger–object collisions and estimate stiffness using intrinsic sensors embedded in standard grippers.

In parallel, bio-inspired soft grippers have been widely studied for manipulating delicate and deformable objects due to their inherent compliance and adaptability [15], [16], [17], [1]. Soft robots can further enhance durability and robustness through mechanisms such as self-healing pneumatic structures [18]. Physics-based modeling approaches have also been explored to estimate contact forces and stiffness in soft robotic grippers. For example, Ghanizadeh et al. [19] employed finite element modeling combined with experimental validation to predict contact forces and enable closed-loop force control. Similarly, Herrera et al. [20] introduced a soft haptic whisker capable of estimating object stiffness through deformation modeling based on Cosserat rod theory while maintaining very low interaction forces.

Due to the inherent compliance and sensing capabilities of pneumatic actuators, pneumatic grippers provide a promising platform for stiffness estimation. In such systems, the relationship between internal pressure, actuator deformation, and object reaction forces can be exploited to infer object stiffness. A stiffness sensing framework using a soft pneumatic gripper performing a pincer grasp was presented in [21], where actuator deformation and pressure signals are used to estimate object stiffness. Similarly, Jang et al. [22] investigated the use of pressure and deformation measurements in pneumatic fingers to infer contact forces and grasp states. Pneumatic actuation has also been utilized to enable variable stiffness manipulation; for example, modulating internal pressure allows soft grippers to adapt their stiffness for different manipulation tasks was demonstrated in [23]. In addition, Grady et al. [24] proposed a visual pressure estimation and control method that infers the pressure applied by a soft gripper using RGB images from an external camera.

These previous studies demonstrate the growing interest in stiffness estimation of soft grippers. In particular, pressure-based sensing in pneumatic grippers provides an effective approach for estimating object stiffness and enabling adaptive grasping.

III. SELF-SENSING HYBRID GRIPPER DESIGN

The proposed self-sensing hybrid gripper consists of three main components: (1) a rigid gripper finger (Fig. 2(b)), (2) a soft ring for air-pressure sensing (Fig. 2(c)), and (3) an compressed air supply and regulation system (Fig. 2(a)). The design details of each subsystem are presented in the following sections.

A. Gripper finger design

The design of this soft-rigid hybrid finger is mainly motivated by the hybrid gripper proposed for grasping paper [25]. The rigid components of the finger, consisting of two links connected by a rotational joint, are comparable in size to an average human finger. Two flange bearings and a rivet screw are integrated into the joint to enable passive backward bending, as shown in Fig. 2(b).

The fingertip can bend up to 80° to facilitate object manipulation. At the bottom of the fingertip, it features a rotatable structure that allows for maintaining consistency in the direction of the normal force applied to the object. Friction within this joint of the structure is minimized by incorporating two bearings and a rivet screw. Both the finger body and the fingertip feature a specialized threading mechanism, shown in Fig. 2(b), that securely anchors the soft ring's fabric layer, enhancing the structural integrity of the hybrid finger.

B. Soft ring design

The soft component of the hybrid gripper, designed in the shape of a ring, provides both adaptability and self-sensing capability when incorporated with a pressure sensor. The design of the soft ring is based on that presented in [25]. It covers the entire finger joint and has an inner diameter of

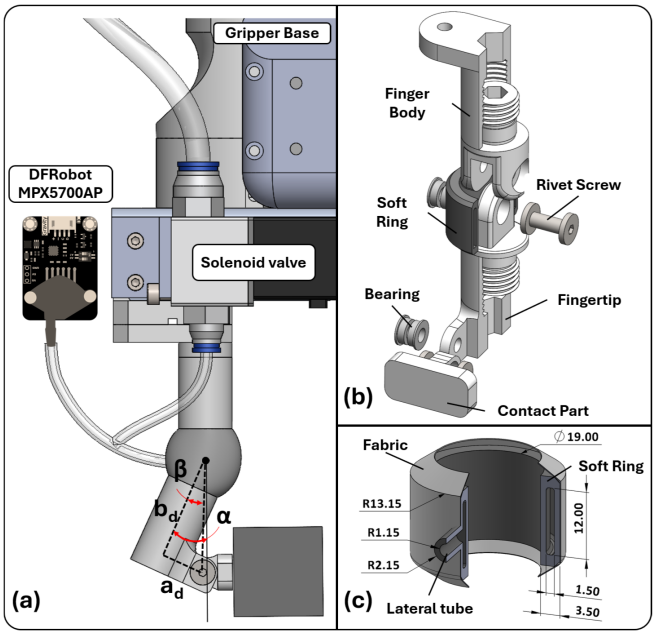


Fig. 2. **Hardware Details:** Structural components and dimensions of the newly designed finger and soft pneumatic system. (a) The pneumatic system consists of a pressure sensor and a soft ring, both controlled through the same air channel connected to a solenoid valve. (b) Cross-sectional view of the hybrid finger showing the newly designed fabric-attaching thread mechanism integrated into the finger body. (c) The drawing illustrates the cross-sectional dimensions of the soft core, which includes an additional tube designed to simplify the installation of the silicone tube.

19 mm and an outer diameter of 26 mm. We added a small lateral tube to accommodate a 4 mm diameter silicone tube that supplies compressed air to the ring. This additional tube simplifies installation and reduces the risk of air leakage.

The soft ring (as shown in Fig. 2(c)) is 3D printed using a Formlabs 3B+ printer with Silicone 40A (Shore A hardness 40). The cavity inside the soft ring is connected with a silicone tube, sealed by Shin-Etsu silicone sealant. A thin layer of non-stretchable chiffon fabric is wrapped and bonded around the soft ring to concentrate the pneumatic pressure onto the finger structure.

C. Gripper's self-sensing pneumatic system

The self-sensing system of the hybrid gripper consists of soft rings that function as actuators, allowing the generation of the grasping force by a passive bending fingertip. With the additional installation of a pressure sensor, the gripper can generate grasping force through pneumatic actuation of the soft rings while simultaneously estimating the object's stiffness by monitoring internal pressure variations during the probing process.

For pressure measurement within the soft ring, an MPX5700AP (DFRobot) pressure sensor module is connected to the ring through an additional air channel arranged in parallel with the soft ring. The sensor is capable of measuring a wide pressure range and has a maximum measurement deviation of approximately 2.5%.

To separately accommodate air volume variations during the operation of the two hybrid fingers, two solenoid valves

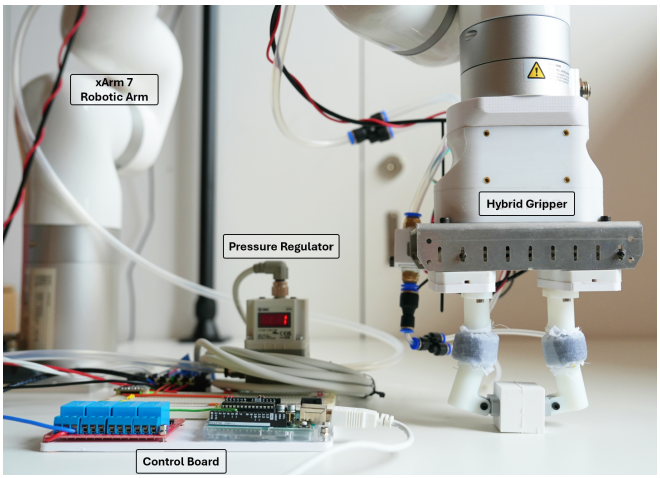


Fig. 3. **System hardware:** Experimental platform comprising an xArm 7 robotic arm equipped with a hybrid gripper, a pneumatic supply line with a pressure regulator (SMC Corporation), and a control board responsible for command generation, signal interfacing, and overall system integration.

are installed upstream of both the soft ring and the pressure sensor within the air channel, shown in Fig. 2(a). These valves isolate and lock the air inside the system, enabling accurate measurement of volume changes.

D. Hardware system, gripper prototype and robot arm

After the fabrication of the soft ring and rigid components is completed, the hybrid fingers are installed into the gripper base. The gripper base is closed-loop controlled by a NEMA17 stepper motor paired with an MKS SERVO42C motor driver, enabling linear inward and outward movement through a solid metal frame.

To facilitate the grasping and probing procedures, the entire hybrid gripper is mounted on a 6-DOF commercial xArm7 robotic arm. This configuration provides the gripper with a high degree of mobility and positional control, allowing it to approach objects from different orientations and perform controlled manipulation tasks. As a result, consistent grasping and probing actions can be executed across different trials, ensuring reliable data collection and improving the overall accuracy of the experimental evaluation conducted in this research.

Regarding the control system, the hybrid gripper is operated by an integrated controller board. The board incorporates a pressure regulator controlled by an MCP4725 12-bit DAC for pneumatic regulation via an Arduino Uno. In addition, an Arduino Nano RP2040 manages the overall system control functions and records data from the pressure sensor.

IV. EXPERIMENTS

A. Soft joint stiffness experiments

1) Soft joint stiffness experiments conducted without air volume constraints: The first experiment is conducted to determine the relationship between the bending angle, compressed air pressure, and the torque exerted at the fingertip. In this experiment, the finger is equipped with a pneumatic system and fixed horizontally on the experimental base using

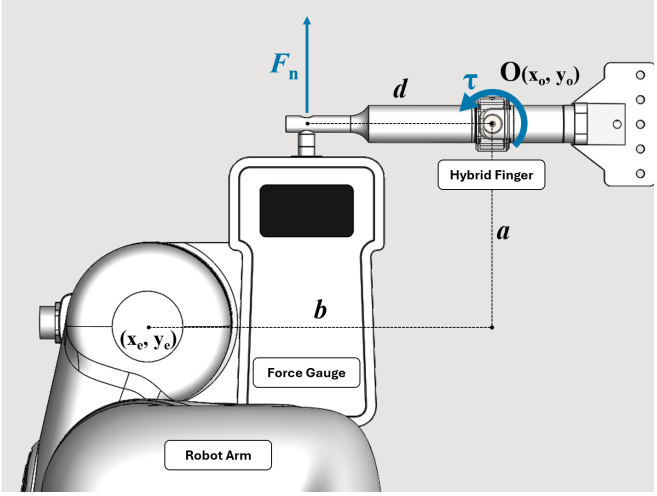


Fig. 4. Demonstration of the data-collection procedure used to validate stiffness estimation. A force gauge mounted on the robot arm follows a circular trajectory around the joint as the fingertip bends. For each bending angle, the torque τ generated by the soft ring is computed from the tangential force F_t and the moment arm length.

a mounting fixture. An Nidec FGP-0.5N force gauge is mounted on the xArm7 robotic arm to generate circular motion in the horizontal plane around the rotation axis of the hybrid finger. The position of the end effector, represented by x_e, y_e, and yaw_e in the O_{xy} plane, can be expressed as a bending angle α about the rotation axis O, located at (x_o, y_o), shown in Fig. 4.

$$\begin{aligned} x_e &= x_o + \sqrt{a^2+b^2}\sin(\alpha-\beta) \\ y_e &= y_o + \sqrt{a^2+b^2}\cos(\alpha-\beta) \\ yaw_e &= yaw_o - \alpha \end{aligned} \tag{1}$$

with a, b, and β being the designed dimension parameters, α is the bending angle of the fingertip, as shown in Fig. 4.

For bending angles from $0°$ to $80°$ with $5°$ increments, and for compressed-air pressure supplied to the soft ring from 0 to 150 kPa in 5 kPa increments, the normal force F_n is recorded using the force gauge at each bending angle, as shown in Fig. 4. Finally, the torque is calculated using the following equation:

$$\tau = F_n d \tag{2}$$

where τ denotes the torque generated by the soft ring at the fingertip, and d represents the length of the experimental fingertip arm. Consequently, the relationship among these three parameters, bending angle, the pressure supplied to the soft ring, and the resulting torque, is illustrated using a heat map in Section V-A

2) Soft joint stiffness experiments with air volume constraints: With the same method conducted in experiment IV-A.1, the relationship between the change in pressure with a fixed amount of air inside the soft ring and the torque generated by the soft ring, paralleled with the bending of the fingertip, is validated.

To completely validate this relationship, for each pressure inside the range from 0 to 100 kPa, both the change in pressure and the torque will be measured according to the bending angle of the fingertip in the same setup in experiment IV-A.1. When the pressure is set to a specific value, the solenoid valve locks the current amount of air inside the ring. With the rotation movement of the force gauge with an angle increment of $1°$ around the axis of the finger joint, the force and the change in pressure would be measured by the force gauge and pressure sensor installed in a parallel air channel with a soft ring.

The reason behind this change in pressure corresponds to the change in the volume of the soft ring. When the bending angle increases, the fingertip will occupy the space, leading to a decrease in the volume inside the soft ring. In addition, the data when the fingertip moves back to the initial position is also recorded to validate the hysteresis characteristic of the hybrid system.

B. Proposed probing method to estimate object stiffness

The primary objective of this method is to estimate the normal force generated when the fingers close inward by a specific distance d_c through the soft ring. Subsequently, the stiffness of the object is determined using the relative stiffness equation based on the estimated normal force.

$$k_r = \frac{F}{d_c} \tag{3}$$

where F is the force estimated by the change of pressure inside the soft ring when contact happens, and d_c is the constant closing distance of the hybrid finger.

The probing process consists of several sequential steps. First, the gripper is fully opened to its maximum range. It is then slowly closed toward the object until initial contact occurs. The contact position is identified by detecting a change in the pressure sensor signal at the moment of contact.

After detecting the initial contact, the gripper advances toward the object with a predefined incremental displacement for five probing times. During each probing time, the change in pressure is measured using the strategies of controlling the initial pressure. These measurements are used to normal contact force F_n. Finally, based on the constant closing displacement of the finger and normal force, the relative stiffness of the objects can be determined and compared with each other.

C. Object stiffness validation experiments

This experiment is conducted to validate the stiffness discrimination capability based on the ground truth value of several objects.

To evaluate the stiffness discrimination capability, there are three different cubes with different stiffness values that would be probed by the hybrid gripper. Among them, two cubes have closely matched stiffness values to evaluate the sensitivity of the system. The ground-truth stiffness value of these objects is obtained by a system of a robot arm and a scale, where the robot arm creates the precise downward movement for the probing head, and the scale measures

the normal force on the cube. The calculated stiffness for objects is presented in Table I. The cubes were fabricated from different materials: Cube 1 was made from Shin-Etsu KE-1415 with a 3% mixing ratio, Cube 2 was made from Shin-Etsu KE-1415 silicone with a 5% mixing ratio, and Cube 3 was made from Formlabs Flexible 80A Resin material.

TABLE I

RELATIVE STIFFNESS OF TESTED OBJECTS

Objects	Relative Stiffness (N/mm)
Cube 1 (20A)	50.83
Cube 2 (30A)	54.87
Cube 3 (80A)	202.39

Afterward, the hybrid gripper sequentially applied the probing method to the sides of the cubes while varying the closing distance and the initial pressure supplied to the soft ring. In this experiment, five different initial pressure values were tested, ranging from $0\,\mathrm{kPa}$ to $80\,\mathrm{kPa}$ with increments of $20\,\mathrm{kPa}$. These conditions are illustrated by five line graphs in Fig. 5. For each initial pressure value, the gripper performed probing with several closing distances.

Based on the results of this experiment, the proposed probing method for distinguishing stiffness between objects using only pressure change measurements has been validated. In addition, the most sensitive pair of parameters (initial pressure and closing distance) for stiffness discrimination can be identified from this experiment, enabling improved performance in real-world grasping and probing tasks in the subsequent experiment.

D. Stiffness probing and grasping experiments

In this experiment, grasping combined with object stiffness estimation in real-world applications is evaluated through the proposed result obtained in the probing method.

A rooted orange or a ripe banana are chosen as the experimental objects. These objects are placed firmly in the experiment's working space. These types of fruits typically exhibit varying levels of stiffness due to non-uniform ripening. To grasp the fruit in this scenario, the gripper must probe and identify areas that are firm enough for secure grasping while avoiding softer, riper regions that could be damaged during manipulation.

To address this issue, the fruit is first placed within the robot's working space. The probing locations are then determined using a hybrid gripper and an appropriate probing strategy based on the fruit's shape. For the orange, the hybrid gripper mounted on a robotic arm rotates its wrist to probe the fruit from multiple angles, ranging from 0° to 180° in steps of 30°. For the banana, the probing process is conducted along its elongated body at ten positions that are equally spaced along the O_y axis of the system.

After collecting the pressure variation data and converting it into the relative stiffness of the object, the hybrid gripper selects the grasping location with the highest stiffness while avoiding softer regions that could damage the fruit.

V. EXPERIMENT RESULTS

A. Soft joint stiffness experiments

1) Soft joint stiffness experiments conducted without air volume constraints: By using Silicone 40A, which has higher Shore Hardness compared with the silicone used in research [25], the stiffness of the joint in this research can go up to $450\,\mathrm{N{\cdot}mm}$ with the bending angle of 80°, as shown in Fig. 6.

Regarding the bending angle range from 0° to 20°, the torque does not change significantly. This result may be attributed to the characteristics of the fabric layer, which loosens at the initial stage of bending and only begins to influence the torque after it is fully stretched beyond 20°.

2) Soft joint stiffness experiments with air volume constraints: Fig. 7 and 8 show that when a constant amount of air is maintained inside the soft ring, the relationship among the torque generated by the soft ring, the initial pressure, and the bending angle is relatively similar to the results obtained in experiment V-A. However, within the bending angle range of 0° to 25°, the looseness of the fabric layer significantly affects the torque generated by the soft ring, resulting in a torque value close to $0\,\mathrm{N{\cdot}mm}$ in this range.

The linear relationship between the change in pressure and the bending angle is noticeable in Fig. 8(b). This result clearly validates the method used to determine the initial contact position during the probing process described in Section IV-B.

In addition, data from the reverse bending process of a specific initial pressure are also recorded in both graphs. The difference between the two colored lines, shown in Fig. 8 and representing the forward and backward bending directions, can be attributed to leakage at the fitting joints in the pneumatic system. Such leakage affects the pressure variation when the solenoid valve attempts to maintain a constant amount of air inside the soft ring.

B. Object stiffness validation experiments

Hooke's law is used to obtain the general stiffness of the object:

$$k_{\mathrm{o}} = \frac{F}{\delta} \tag{4}$$

Furthermore, the deformation of the object along the x-axis can be calculated using the following equation for the given configuration of the hybrid gripper, corresponding to the bending angle α:

$$\delta = d_{\mathrm{c}} - (a_d + \sqrt{a_d^2 + b_d^2}\sin(\alpha - \beta_d)) \tag{5}$$

with a_d and b_d being the designed dimension parameters of the hybrid finger length, and β_d is the designed angle of the finger, as shown in Fig. 2.

From Fig. 7, we observe that the bending angle is directly proportional to both the pressure change and the torque generated by the soft ring. This relationship validates the use of equation (3) for estimating the relative stiffness of the objects.

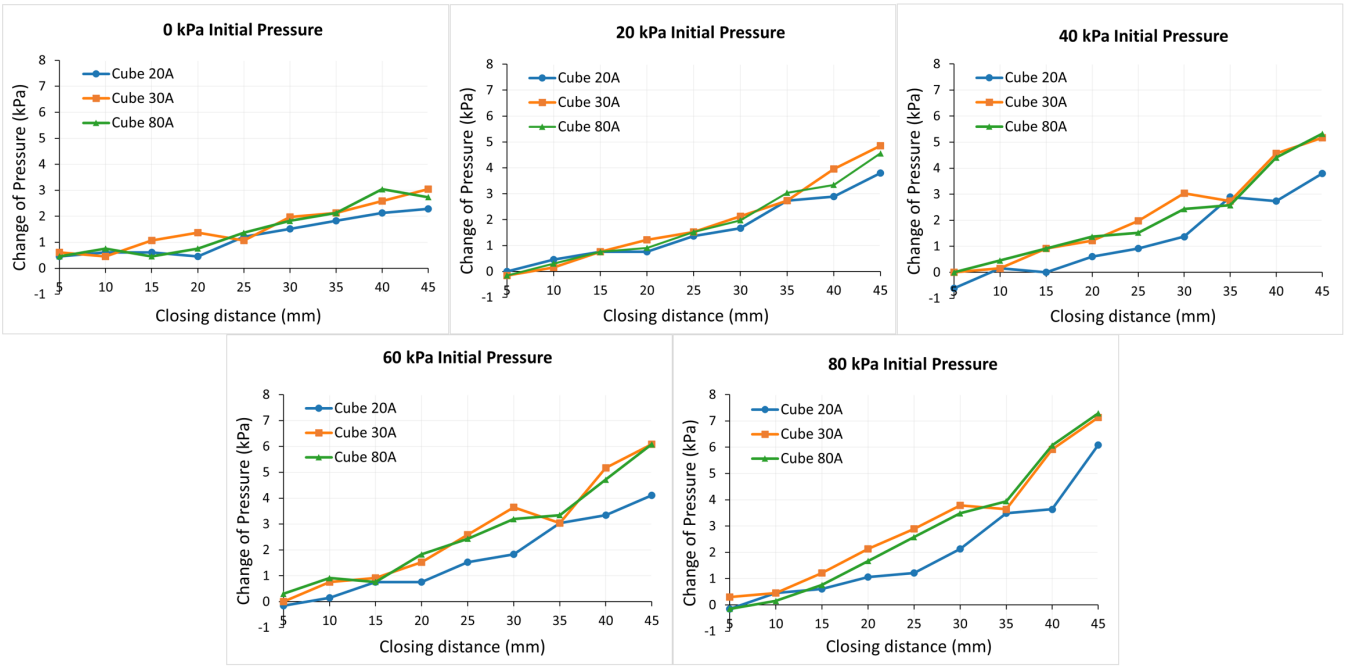


Fig. 5. Pressure variation during the probing process under different initial pressures. Each subplot shows the relationship between the change in pressure and the gripper closing distance for objects with different stiffness levels (Cube 20A, Cube 30A, and Cube 80A). As the closing distance increases, the pressure change becomes more significant for stiffer objects, demonstrating that pressure variation can be used to distinguish relative object stiffness. In addition, the gripper demonstrates higher sensitivity in differentiating stiffness at an initial pressure of 60 kPa and a closing distance of approximately 30 mm.

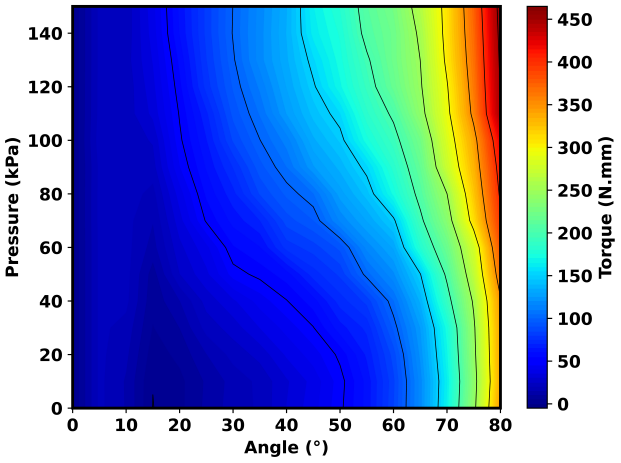


Fig. 6. The torque was measured in soft-joint stiffness experiments, with pressure continuously controlled by a regulator from 0 to 150 kPa and bending angles ranging from 0° to 80°.

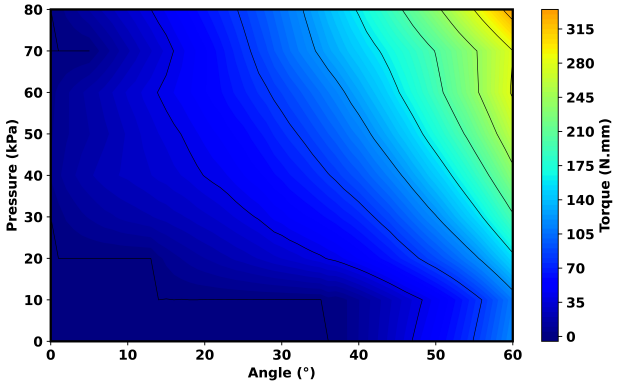


Fig. 7. The torque was measured in soft-joint stiffness experiments under constrained air-volume conditions by solenoid valves, with bending angles ranging from 0° to 60° and pressures ranging from 0 to 80 kPa.

In addition, the deformation of the object is inversely proportional to the bending angle of the fingertip after contact happens, as implied by equation (5). Therefore, based on the standard formula for the stiffness of the object presented in equation (4), we can conclude that the stiffness of the object is directly proportional to the pressure change of the soft ring. This result indicates that measuring the pressure change after probing an object with this hybrid gripper is sufficient to distinguish the relative stiffness between different objects.

C. *Stiffness probing and grasping experiments*

In this experiment, the proposed probing method is applied to measure pressure changes in order to infer the relative stiffness at defined positions on the bodies of a banana and an orange.

Fig. 9 indicates the variation in pressure change along the body of the banana. From position 0 to 70 mm, the pressure change is not noticeable. However, at positions 80 mm and 90 mm, denoted by red marks, the pressure change is significantly lower, indicating that the stiffness at these positions is lower than at the others. Similar to the banana probing process, the hybrid gripper identifies locations with lower pressure changes after rotating to probe around the orange at 30°, 60°, and 90°. Based on these data, the possible

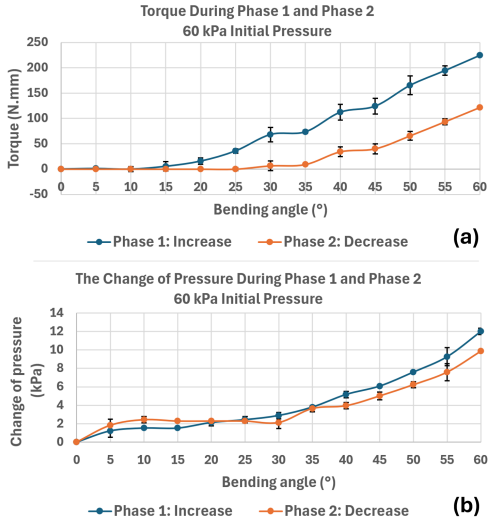


Fig. 8. (a) Torque–bending angle relationship during Phase 1 (increasing) and Phase 2 (decreasing). (b) Corresponding pressure variation as a function of bending angle for both phases. In Phase 1, data were recorded as the fingertip bent progressively from 0° to a specified angle. In Phase 2, data were recorded as the fingertip bent to a maximum angle of 60° and then returned to the specified angle, where measurements were taken.

grasping locations for both fruits are indicated by green marks, where the stiffness is estimated to be higher than at the locations marked in red.

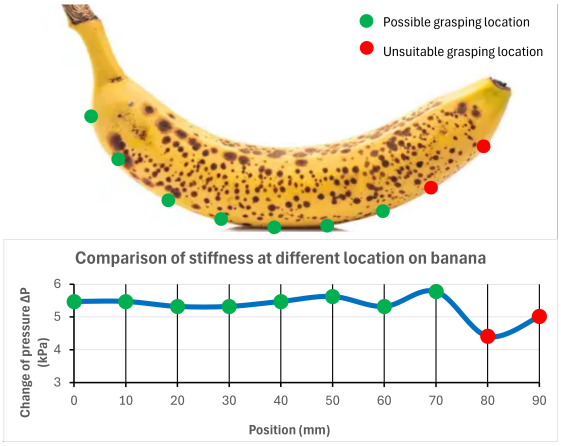


Fig. 9. The relative stiffness of the banana was measured at different positions along its length. The softest region coincided with the black spot on the peel.

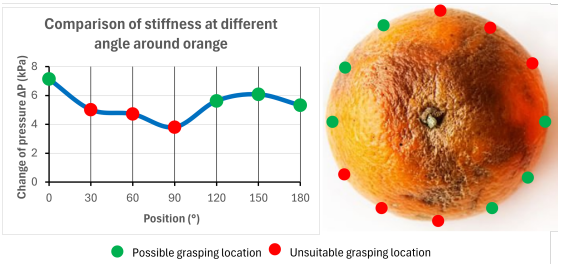


Fig. 10. The relative stiffness of the semi-rooted orange was measured at different positions around its center. Based on these results, the orange should be grasped at the position with the highest stiffness to ensure a stable grip.

VI. LIMITATIONS & FUTURE WORK

Although the proposed hybrid gripper demonstrates the capability to estimate the relative stiffness of objects through pressure variation, several limitations remain in the current system. First, the pressure sensor used in the system has relatively low resolution, which limits the accuracy of pressure change measurements during the probing process. This limitation could be addressed in future work by integrating a higher-resolution pressure sensor. In addition, hysteresis effects in the soft material, as well as unavoidable air leakage at the pneumatic fitting joints, may affect the repeatability and consistency of the measurements. Furthermore, the pressure sensor is currently installed on only one fingertip of the gripper, which restricts the sensing capability during multi-contact interactions.

Future work will focus on addressing these limitations and improving the overall performance of the system. In particular, simulation software will be employed to thoroughly validate the proposed sensing principle and to analyze the deformation behavior of the soft ring under different loading conditions. These simulations will facilitate optimization of the structural design and sensing parameters of the hybrid gripper, thereby improving the accuracy, sensitivity, and robustness of stiffness estimation.

VII. CONCLUSIONS

This paper presented a probe-to-grasp manipulation framework built around a passive pneumatic hybrid gripper with self-sensing, variable-stiffness joints. By integrating rigid finger links with a soft pneumatic ring at each joint, the gripper achieves compliant interaction while allowing joint stiffness to be tuned through internal pressure. Instead of relying on embedded tactile or force sensors, we leveraged a single pressure sensor together with an experimentally identified lookup relationship between joint bending, pressure variation under constrained air volume, and the resulting joint torque. This enables practical estimation of contact forces during probing and grasping using minimal hardware. While the proposed approach offers a low-cost and easily deployable alternative to traditional tactile sensing, accuracy and repeatability can be further improved by addressing pressure sensor resolution. Future work will also include simulation-based analysis of soft ring deformation to optimize structural and sensing parameters and improve robustness across a broader range of objects and contact conditions.

REFERENCES

[1] J. Shintake, V. Cacucciolo, D. Floreano, and H. Shea, "Soft robotic grippers," *Advanced materials*, vol. 30, no. 29, p. 1707035, 2018.

[2] Y. Fan, B. Yi, and D. Liu, "An overview of stiffening approaches for continuum robots," *Robotics and Computer-Integrated Manufacturing*, vol. 90, p. 102811, 2024.

[3] X. Yang, H. Ren, D. Guo, Z. Ling, T. Zhang, G. Li, Y. Tang, H. Zhao, J. Wang, H. Chang *et al.*, "A soft tactile unit with three-dimensional force and temperature mathematical decoupling ability for robots," *Engineering*, vol. 55, pp. 96–106, 2025.

[4] H. Li, H. Niu, F. Yin, W. Zhou, G. Shen, and Y. Li, "A labor-division cooperation electronic palm system for high-precision crosstalk-free cognition of pressure and temperature," *Advanced Materials*, vol. 38, no. 8, p. e10241, 2026.

[5] J. Ji, H. Luo, J. Su, S. Wang, X. Chen, and J. Song, "Multisensory electronic skin with decoupled pressure–temperature-sensing capabilities for similar object recognition," *Proceedings of the National Academy of Sciences*, vol. 122, no. 41, p. e2519693122, 2025.

[6] Z. Liu, X. Hu, R. Bo, Y. Yang, X. Cheng, W. Pang, Q. Liu, Y. Wang, S. Wang, S. Xu *et al.*, "A three-dimensionally architected electronic skin mimicking human mechanosensation," *Science*, vol. 384, no. 6699, pp. 987–994, 2024.

[7] K. Chin, T. Hellebrekers, and C. Majidi, "Machine learning for soft robotic sensing and control," *Advanced Intelligent Systems*, vol. 2, no. 6, p. 1900171, 2020.

[8] P. Wang, L. Wang, R. Chen, J. Xu, J. Xu, and M. Gao, "Overview and outlook on railway track stiffness measurement," *Journal of Modern Transportation*, vol. 24, no. 2, pp. 89–102, 2016.

[9] G. Hattori and A. L. Serpa, "Contact stiffness estimation in ansys using simplified models and artificial neural networks," *Finite Elements in Analysis and Design*, vol. 97, pp. 43–53, 2015.

[10] Y. Gao, L. A. Hendricks, K. J. Kuchenbecker, and T. Darrell, "Deep learning for tactile understanding from visual and haptic data," in *2016 IEEE international conference on robotics and automation (ICRA)*. IEEE, 2016, pp. 536–543.

[11] M. Bednarek, P. Kicki, J. Bednarek, and K. Walas, "Gaining a sense of touch object stiffness estimation using a soft gripper and neural networks," *Electronics*, vol. 10, no. 1, p. 96, 2021.

[12] Z. He, B. Lian, and Y. Song, "Rigid-soft coupled robotic gripper for adaptable grasping. j bionic eng 20: 2601–2618," 2023.

[13] F. J. Ruiz-Ruiz, J. Ventura, C. Urdiales, and J. M. Gómez-de Gabriel, "Compliant gripper with force estimation for physical human–robot interaction," *Mechanism and Machine Theory*, vol. 178, p. 105062, 2022.

[14] S. Cortinovis, M. Maggiali, and R. A. Romeo, "Stiffness estimation and finger-object impact detection with a robotic gripper using intrinsic sensors," *Sensors and Actuators A: Physical*, vol. 388, p. 116463, 2025.

[15] L. U. Odhner, R. R. Ma, and A. M. Dollar, "Open-loop precision grasping with underactuated hands inspired by a human manipulation strategy," *IEEE Transactions on Automation Science and Engineering*, vol. 10, no. 3, pp. 625–633, 2013.

[16] S. Li, J. J. Stampfli, H. J. Xu, E. Malkin, E. V. Diaz, D. Rus, and R. J. Wood, "A vacuum-driven origami "magic-ball" soft gripper," in *2019 International Conference on Robotics and Automation (ICRA)*. IEEE, 2019, pp. 7401–7408.

[17] M. Manti, T. Hassan, G. Passetti, N. D'Elia, C. Laschi, and M. Cianchetti, "A bioinspired soft robotic gripper for adaptable and effective grasping," *Soft Robotics*, vol. 2, no. 3, pp. 107–116, 2015.

[18] S. Terryn, J. Brancart, D. Lefeber, G. Van Assche, and B. Vanderborght, "Self-healing soft pneumatic robots," *Science Robotics*, vol. 2, no. 9, p. eaan4268, 2017.

[19] A. Ghanizadeh, F. Ghanbili, and A. Bahrami, "Contact force estimation and control in soft fin-ray grippers using fem and experimental approach," in *2024 12th RSI International Conference on Robotics and Mechatronics (ICRoM)*. IEEE, 2024, pp. 076–082.

[20] L. Herrera-Ubaldo, J. P. Espejel Flores, L. Soriano, G. Cielniak, L. Guevara, and A. Yilmaz, "Physically realistic digital replica of strawberry plants for robotic harvesting," in *Innovative Agricultural Technologies Congress*. Springer, 2025, pp. 111–127.

[21] C. Sithiwichankit and R. Chancharoen, "Advanced stiffness sensing through the pincer grasping of soft pneumatic grippers," *Sensors*, vol. 23, no. 13, p. 6094, 2023.

[22] H. Jang, J. Bae, and K. Haninger, "Soft finger grasp force and contact state estimation from tactile sensors," *arXiv preprint arXiv:2410.19684*, 2024.

[23] Z. Song, Z. Wang, B. Liu, Y. Song, and X. Zhang, "A soft gripper based on pneunets structure with stiffness-variable-enhanced load capacity for object grasping," *Sensors and Actuators A: Physical*, vol. 383, p. 116253, 2025.

[24] P. Grady, J. A. Collins, S. Brahmbhatt, C. D. Twigg, C. Tang, J. Hays, and C. C. Kemp, "Visual pressure estimation and control for soft robotic grippers," in *2022 IEEE/RSJ International Conference on Intelligent Robots and Systems (IROS)*. IEEE, 2022, pp. 3628–3635.

[25] N. D. Tran, H. H. Ly, X. T. Nguyen, T. T. Mac, A. Nguyen, and T. D. Ta, "Hybrid gripper with passive pneumatic soft joints for grasping deformable thin objects," *Proceedings - IEEE International Conference on Robotics and Automation*, pp. 7858–7864, 2025.